Research article

The role of delay in vaccination rate on Covid-19

Mohammed Salman [a], Sanjay Kumar Mohanty [a,*], Chittaranjan Nayak [b], Sachin Kumar [c,*]

[a] *Department of Mathematics, SAS, Vellore Institute of Technology, Vellore, 632014, Tamil Nadu, India*
[b] *Department of Communication Engineering, School of Electronics Engineering, Vellore Institute of Technology, Vellore, 632014, Tamil Nadu, India*
[c] *Department of Electronics and Communication Engineering, SRM Institute of Science and Technology, Kattankulathur, 603203, Tamil Nadu, India*

ARTICLE INFO

ABSTRACT

The role of vaccination in tackling Covid-19 and the potential consequences of a time delay in vaccination rate are discussed. This study presents a mathematical model that incorporates the rate of vaccination and parameters related to the presence and absence of time delay in the context of Covid-19. We conducted a study on the global dynamics of a Covid-19 outbreak model, which incorporates a vaccinated population and a time delay parameter. Our findings demonstrate the global stability of these models. Our observation indicates that lower vaccination rates are associated with an increase in the overall number of infected individuals. The stability of the corresponding time delay model is determined by the value of the time delay parameter. If the time delay parameter is less than the critical value at which the Hopf bifurcation occurs, the model is stable. The results are supported by numerical illustrations that have epidemiological relevance.

1. Introduction

The rapid spread of the Covid-19 pandemic and other global epidemics has accomplished infectious disease research increasingly important in recent decades. The observed data [Fig. 3] show that the vaccinated population has a significant impact on disease transmission rates, but there is limited research evidence to back up this claim. Understanding the mathematical models and simulations used to evaluate the effectiveness of vaccination against infectious diseases such as Covid-19 is crucial. Mathematical modelling of infectious disease is a prevalent area of study these times, due to its effective way of forecasting infections. Using an ordinary differential equation, Kermack and McKendrick [1] described the model for infectious diseases in SIR and presented the solution. P Van den Driessche [2] discovered that the value of the basic reproduction number for a specific disease is influenced by a variety of variables, including place and population density. If the basic reproduction number is less than one, the disease is eliminated. Again, if it is larger than one, the disease continues to spread. Hassan et al. [3] proposed a model for Covid-19 in Texas to predict the upcoming infection rate and probability of outbreak using the basic reproduction number. Kribs-Zaleta et al. [4] proposed a two-population dynamical model and observed the effects of vaccination. Mpinganzima et al. [5] investigated the Covid-19 model to know the positive effects of government-implemented control measures in Rwanda. Okuonghae and Omame [6] investigated the impact of the pharmaceutical measure, specifically, face masks, social distancing and case detention on Covid-19. Mwangi et al. [7] proposed a mathematical model of Covid-19 in Kenya and concluded that mass vaccination, early detection of infection, and contact

tracing are factors in disease control. Watson et al. [8] estimated the effect of vaccination in several countries using statistical data and suggested that vaccination campaigns had saved millions of lives, but rather distributing vaccines earlier might be more effective.

In describing the severity of a pandemic, the stability of disease free equilibrium plays a major role. Shuai et al. [9] developed different Lyapunov functions for general infectious disease and demonstrated the matrix-theoretic method for disease free equilibrium stability and the graph-theoretic method for endemic equilibrium stability. Kammegne et al. [10] analyzed the global stability of Covid-19 model using Routh-Horwitz criterion. De Leenheer et al. [11] considered a positive linear system to demonstrate that if all the eigenvalues of the linearized system are negative, there exists a stable equilibrium and also, provided the necessary and sufficient conditions to solve the system. Using a vaccination model, Guan et al. [12] demonstrated the global stability of the endemic equilibrium. Omame et al. [13] studied the impact of the Pfizer, Moderna and Janssen Vaccine for the city of Texas, United States of America. Ojo et al. [14] studied the effect of co-dynamics associated with Covid-19 and tuberculosis in the population and discussed the stability of both diseases. Omame and Abbas [15] discussed the asymptotic stability of a co-dynamical model with patients infected with both SARS-Cov-2 and HBV. The stochastic version of mathematical model for Covid-19 is discussed in [16–18].

It is essential to understand the consequences that come with time delay for the deterministic models of infectious disease. A time delay must be introduced to comprehend the possibility that the stability of the equilibria could modify. Tyagi et al. [19] investigated the deterministic model with a corresponding delay model. Meng et al. [20] considered the time delay SEIR model for epidemics with vertical transmission and studied the dynamic behaviour of the model. Röst [21] created an SEIR model with infectivity varying over disease age along an infinite distributed delay and demonstrated the global stability of the equilibrium using a threshold quantity. Xu et al. [22] analysed an SEIRS model for epidemics with time delay in the latent period. Dagasso et al. [23] investigated a mathematical model for infectious disease based on differential equations with delayed vaccination responses and described potential immunisation reactions in SARS-Cov-2.

The article is structured as follows. The mathematical model of Covid-19 with vaccination is discussed in section 2. In section 3, we examined the model's stability by constructing an appropriate Lyapunov function through the next-generation matrix technique. The time delay system is covered in two subsections in section 4. The numerical outcomes for studying the influence of various threshold parameters on deterministic, and time delay models are analyzed in section 5. The effect of vaccination is then summarized, and conclusions are drawn.

2. The model formulation

Assume that N is the size of the population at time t, and it is divided into four sub-classes as follows: susceptible population(S), asymptomatic population(A), infected population with symptoms(I), and vaccinated people(V). Susceptible individuals(S) become infected through sufficient contact with infected individuals(I) or asymptomatic individuals(I) [24,25], the proportion of susceptible people that become asymptomatic or infected is β. Once infected, they shift to either the asymptomatic compartment(A) or the symptomatic compartment(I), and it is believed that vaccinated individuals are safe as long as they stay in the vaccinated compartment. The infected individual, whether asymptomatic or infected with symptoms, will revert to susceptible at γ_1 and γ_2 rates. The birth rate and natural death rate are Λ and δ, respectively, φ is the rate for vaccination of susceptible individuals, γ_3 is the vaccine failure rate, λ is the rate for shifting of asymptomatic individuals to the infected compartment, q is the probability that a susceptible person has influenza immunity, and μ is the ratio for susceptible individuals moving to asymptomatic. We have the SAIV compartmental model as shown below [12]:

$$
\begin{aligned}
\frac{dS}{dt} &= (1-q)\Lambda - \delta S - \varphi S - \beta S(I + \mu A) + \gamma_1 A + \gamma_2 I + \gamma_3 V, \\
\frac{dA}{dt} &= \mu \beta S A - \delta A - \lambda A - \gamma_1 A, \\
\frac{dI}{dt} &= \beta S I + \lambda A - \delta I - \gamma_2 I, \\
\frac{dV}{dt} &= q\Lambda + \varphi S - \delta V - \gamma_3 V.
\end{aligned}
\tag{1}
$$

The assumption includes the rates being constant, and the initial conditions are $S(t)$, $A(t)$, $I(t)$ & $V(t) > 0$. Disease free equilibrium (DFE) is defined for the system in equation (1) as $E_d = (S_d, A_d, I_d, V_d)$ and the endemic equilibrium $E_i = (S_i, A_i, I_i, V_i)$. The following result is established to show the global attractive region of the system in equation (1).

Theorem 1. *The solutions of system in equation (1) are positively invariant.*

Proof. To prove the system in equation (1) is positively invariant, we consider the total population as $N(t)$ with $N(0) = \frac{\Lambda}{\delta}$ and define

$$N(t) = S(t) + A(t) + I(t) + V(t).$$

From the non-negativity of the solutions associated with susceptible, asymptomatic, infectious and vaccination compartments, follows that

$$\frac{dN}{dt} = \Lambda - \delta N,$$

and implies

$$N = \frac{\Lambda}{\delta}.$$

From the above it is concluded that $N(t)$ is bounded and hence $S(t)$, $A(t)$, $I(t)$ and $V(t)$.

Therefore, the global attractor of the system in equation (1) is defined by

$$\Gamma = \left\{ (S, A, I, V) \in \mathbf{R}_+^4 : S + A + I + V = \frac{\Lambda}{\delta} \right\},$$

is positively invariant. $\square$

Next, we have derived DFE of the system in equation (1) as $E_d = (S_d, 0, 0, V_d)$, with

$$S_d = \frac{\Lambda \left(\delta(1-q) + \gamma_3 \right)}{\delta \left(\delta + \varphi + \gamma_3 \right)}, \quad V_d = \frac{\Lambda(\delta q + \varphi)}{\delta \left(\delta + \varphi + \gamma_3 \right)}.$$

3. Basic reproduction number and global stability near DFE

In this section, the Lyapunov function is constructed to prove the global stability at DFE. In a community where everyone is susceptible to becoming infected, the basic reproduction number (R_0) is the predicted number of secondary infections induced by a single infectious person. To determine R_0, we applied a next-generation matrix method described in [26]. We recast the equations for asymptomatic and infectious compartments of the system in equation (1) as

$$\frac{dX_i}{dt} = \mathcal{F}_i - \mathcal{V}_i, \quad i = 1, 2,$$

where X_1 is the asymptomatic and X_2 is the infected individuals with $\mathcal{F}_i$ and $\mathcal{V}_i$ is the rates of collection that cause new infectious individuals and the collection of rates related to the movement of infected individuals among the uninfected, respectively. Here, the collections $\mathcal{F}_i$ and $\mathcal{V}_i$ are given as

$$\mathcal{F} = \begin{pmatrix} \mu \beta S A \\ \beta S I \end{pmatrix} \text{ and } \mathcal{V} = \begin{pmatrix} \delta A + \lambda A + \gamma_1 A \\ -\lambda A + \delta I + \gamma_2 I \end{pmatrix}.$$

The spectral radius of the next generation matrix FV^{-1} is the basic reproduction number with F and V as Jaccobian of $\mathcal{F}$ and $\mathcal{V}$, respectively at DFE and are given by

$$F = \begin{pmatrix} \frac{\beta \mu \Lambda \left(\delta(1-q) + \gamma_3 \right)}{\delta(\delta + \varphi + \gamma_3)} & 0 \\ 0 & \frac{\beta \Lambda \left(\delta(1-q) + \gamma_3 \right)}{\delta(\delta + \varphi + \gamma_3)} \end{pmatrix}, \quad V = \begin{pmatrix} \delta + \lambda + \gamma_1 & 0 \\ -\lambda & \delta + \gamma_2 \end{pmatrix},$$

and

$$FV^{-1} = \begin{pmatrix} m_{11} & m_{12} \\ m_{21} & m_{22} \end{pmatrix},$$

with

$$m_{11} = \frac{\beta \Lambda \mu \left(\delta(1-q) + \gamma_3 \right)}{\delta \left(\delta + \varphi + \gamma_3 \right) \left(\delta + \lambda + \gamma_1 \right)},$$

$$m_{12} = 0,$$

$$m_{21} = \frac{\beta \Lambda \left(\delta(1-q) + \gamma_3 \right) \lambda}{\delta \left(\delta + \varphi + \gamma_3 \right) \left(\delta + \lambda + \gamma_1 \right) \left(\delta + \gamma_2 \right)},$$

and

$$m_{22} = \frac{\beta \Lambda \left(\delta(1-q) + \gamma_3 \right)}{\delta \left(\delta + \varphi + \gamma_3 \right) \left(\delta + \gamma_2 \right)}.$$

We have derived the spectral radius

$$R_0 = \rho \left(FV^{-1} \right) = \frac{\Lambda \beta \mu \left(\delta(1-q) + \gamma_3 \right)}{\delta \left(\delta + \varphi + \gamma_3 \right) \left(\delta + \lambda + \gamma_1 \right)}.$$

The derived R_0 is used to analyze the existence of endemic equilibrium. Essentially establishing a suitable Lyapunov function, we obtain a subsequent global stability outcome near the DFE.

Theorem 2. *If $R_0 < 1$ then the DFE $(S_d, 0, 0, V_d)$ of system in equation (1) is globally asymptotically stable in R^{4+}.*

Proof. : To prove the global stability of the system in equation (1), let's define a Lyapunov function $L_1 = L_1(S, A, I, V)$ such that

$$L_1 : \mathbb{R}^{4^+} \to \mathbb{R}$$

and

$$L_1 = C_0 \left[\frac{\Lambda \beta \mu (\delta(1-q) + \gamma_3)}{\delta C_0 C_1 C_2} \int_0^t A \, dt + \frac{A}{C_0 C_2} + \int_0^t I \, dt + \frac{I}{(\delta + \gamma_2)} \right],$$

where $C_1 = \delta + \varphi + \gamma_3$, $C_2 = \delta + \gamma_1 + \lambda$ and C_0 is positively chosen constant. It can be easily verified that $L_1(S_d, 0, 0, V_d) = 0$ and $L_1(S, A, I, V) > 0$. The derivative of L_1 can be obtained as

$$
\begin{aligned}
\frac{dL_1}{dt} &= C_0 \left[\frac{\Lambda \beta \mu (\delta(1-q) + \gamma_3)}{\delta C_0 C_1 C_2} A + \frac{\dot{A}}{C_0 C_2} + I + \frac{\dot{I}}{(\delta + \gamma_2)} \right] \\
&= \left[\frac{\Lambda \beta \mu (\delta(1-q) + \gamma_3)}{\delta C_1 C_2} - 1 \right] A + C_0 \left[\frac{\mu \beta S A}{C_0 C_2} + \frac{\beta S I}{(\delta + \gamma_2)} + \frac{\lambda A}{(\delta + \gamma_2)} \right] \\
&= \left[R_0 - 1 \right] A + C_0 \left[\frac{\mu \beta S A}{C_0 C_2} + \frac{\beta S I}{(\delta + \gamma_2)} + \frac{\lambda A}{(\delta + \gamma_2)} \right].
\end{aligned}
$$

Hence, it is easy to see $\frac{dL_1}{dt} < 0$, whenever R_0 less than one with appropriately chosen C_0. Since C_0 is very small, the product $C_0 \left(\frac{\beta S I}{(\delta + \gamma_2)} + \frac{\lambda A}{(\delta + \gamma_2)} \right)$ does not have an impact on changing the sign of first term. ☐

If $\mathcal{R}_0 < 1$, the DFE is stable globally asymptotically in Γ. Again, if $\mathcal{R}_0 > 1$, DFE becomes unstable, and the endemic equilibrium is stable globally asymptotically in Γ. We have seen that the following conditions hold for the existence of an endemic equilibrium of the system in equation (1):

$$\mu > \frac{\delta + \lambda + \gamma_1}{\delta + \gamma_2}, \quad \frac{\Lambda}{\delta} > \frac{(\mu \beta S A + \delta + \lambda + \gamma_1)(\delta + \varphi + \gamma_3)}{\beta \mu (\delta(1-q) + \gamma_3)} \text{ and } \mathcal{R}_0 > 1.$$

Again, the endemic equilibrium of system in equation (1) is obtained as $E_i = (S_i, A_i, I_i, V_i)$, with

$$S_i = \frac{\delta + \lambda + \gamma_1}{\beta \mu},$$

$$I_i = \frac{\mu \lambda A^*}{\mu(\delta + \gamma_2) - (\delta + \lambda + \gamma_1)},$$

$$A_i = \left(\delta a_1 a_2 (R_0 - 1) + \beta \mu (\gamma_3 + (1-q)\delta) \right) \left(\frac{a_1 a_2}{\beta \mu (\gamma_3 + \delta) R_0} \right),$$

$$V_i = \frac{\Lambda q \beta \mu + \varphi(\delta + \lambda + \gamma_1)}{\beta \mu (\delta + \gamma_3)},$$

where $a_1 = \gamma_3 + \delta + \varphi$ and $a_2 = \gamma_1 + \delta + \lambda$. Small perturbations associated with the rate of infections are examined in the next section.

4. The delayed model

In this section, we examine the Hopf bifurcation and global stability for system in equation (1) with a time delay parameter. The incorporation of the time delay parameter in an ordinary differential system will replicate the number of infected individuals precisely for certain viral infections in the human body. A time delay for a differential equation system is an essential tool in several population interaction models. The Hopf bifurcation is a local disturbance in the stability analysis of a fixed point that results in the emergence or extinction of a periodic orbit. The stability of the system switches at the Hopf bifurcation, which is a crucial point where a periodic solution occurs. We split the corresponding delayed model of the system in equation (1) as SAI delay model and SV delay model for simplicity and the same are discussed in the subsections.

4.1. SAI delay model

The SAI delay model is framed to understand the behaviour of the susceptible, asymptomatic, and infectious populations with a time delay parameter associated with the rate of infection. We include the time delay parameter ($\tau > 0$) to acquire precise results of the system in equation (1), and is given by

$$
\begin{aligned}
\frac{dS}{dt} &= \Lambda - \delta S - \varphi S - \beta S(I(t - \tau) + \mu A(t - \tau)), \\
\frac{dA}{dt} &= \mu \beta S A(t - \tau) - \delta A - \lambda A, \\
\frac{dI}{dt} &= \beta S I(t - \tau) + \lambda A - \delta I.
\end{aligned}
\tag{2}
$$

It is essential to provide an initial condition to define the value of the solution prior to time $t = 0$. Here, the initial conditions are $S_0(\theta) = \phi_1(\theta) > 0$, $A_0(\theta) = \phi_2(\theta) > 0$, $I_0(\theta) = \phi_3(\theta) > 0$, with $\theta \in [-\tau, 0]$. Here, $\phi_i \in C\left([-\tau, 0] \to \mathbb{R}_+\right)$, $i = 1, 2, 3$ are known functions. In the vector form, we can rewrite the system in equation (2) by setting $X \in (S, A, I)^T \in \mathbb{R}^3$ and

$$G(X) = \begin{pmatrix} G_1(X) \\ G_2(X) \\ G_3(X) \end{pmatrix} = \begin{pmatrix} \Lambda - \delta S - \varphi S - \beta S(I(t-\tau) + \mu A(t-\tau)) \\ \mu \beta S A(t-\tau) - \delta A - \lambda A \\ \beta S I(t-\tau) + \lambda A - \delta I \end{pmatrix},$$

where $G : C_+ \to \mathbb{R}^3$ and $G \in C^\infty\left(\mathbb{R}^3\right)$. Hence, the delayed system in equation (2) becomes

$$\frac{dX_t(t)}{dt} = G\left(X_t\right),$$

where $X_t(\theta) = X(t + \theta)$. The following theorem concerns the biologically feasible region of the delayed system in equation (2).

Theorem 3. *The solutions of delayed system in equation (2) are positively invariant.*

Proof. To prove the system in equation (2) is positively invariant, we consider the total population as B(t), and we define

$$B(t) = S(t) + A(t) + I(t).$$

From the non-negativity of the solutions associated with susceptible, asymptomatic, and infectious compartments it follows that

$$\frac{dB}{dt} = \Lambda - b(S(t) + A(t) + I(t)) \leq \Lambda - bB(t),$$

with $b = \min\{\delta + \varphi, \delta \pm \lambda\}$. This indicates that $B(t)$ is bounded, therefore the biologically feasible region of delayed system in equation (2) is defined by

$$\Omega = \left\{(S, A, I) \in \mathbb{R}_+^3 : S, I, A \geq 0\right\},$$

is positively invariant. $\quad\square$

Next, we determine the sufficient condition for the parameters to ensure the stability of the disease free and endemic steady state of the system in equation (2).

Theorem 4. *For $\tau \geq 0$, the disease free steady state of the delayed system in equation (2) is linearly asymptotically stable.*

Proof. To prove the asymptotic stability of the disease free steady state of the delayed system in equation (2) using the Routh-Hurwitz criterion. Let J1 denote the Jacobian of the delayed system in equation (2) at the steady state $E_* = (S^*, A^*, I^*)$. Upon linearizing the system in equation (2) at J1 = 0, we get

$$\begin{vmatrix} u_1 - x & -\beta S^* \mu e^{-x\tau} & -\beta S^* e^{-x\tau} \\ \beta A^* \mu e^{-x\tau} & u_2 - x & 0 \\ \beta I^* \mu e^{-x\tau} & \lambda & u_3 - x \end{vmatrix} = 0, \tag{3}$$

where $u_1 = -(\delta + \varphi + \beta(I^* + \mu A^*))$, $u_2 = \mu \beta S^* - (\delta + \lambda)$ and $u_3 = \beta S^* - \delta$. We have derived the characteristic polynomial in equation (3) as

$$x^3 + U_1 x^2 + U_2 x + U_3 + e^{-2x\tau}\left(Q_1 x + Q_2\right) = 0,$$

with

$$U_1 = (I^* - S^* + (A^* - S^*)\mu)\beta + 3\delta + \varphi + \lambda,$$

$$U_2 = (2\delta - S^*\beta\mu + \lambda - S^*\beta)\beta\mu A^* + (2\delta + \lambda - S^*\beta - S^*\beta\mu)\beta I^* + ((\beta S^* - 2\delta - \varphi) - 2\delta - \varphi - \lambda - 2\mu\delta - \mu\varphi)S^*\beta + 2\delta\varphi + 2\delta\lambda + \varphi\lambda + 3\delta^2,$$

$$U_3 = [A^*\beta\mu(S^*\beta - \delta)(S^*\beta\mu - \lambda - \delta)] + [I^*\beta(S\beta - \delta)(S\beta\mu - \lambda - \delta)] + [S^*\beta(\delta + \varphi)(S^*\beta\mu - \lambda - \mu\delta - \delta)] + [\delta(\delta + \lambda)(\delta + \varphi)],$$

$$Q_1 = S^*\beta^2(A^*\mu^2 + I^*),$$

$$Q_2 = S^*\beta^2((\delta + \lambda - S^*\beta\mu)I^* + (\mu\lambda + \mu^2\delta - S^*\beta\mu^2)A^*).$$

The following system of equation can be derived if the characteristic polynomial in equation (3) has purely imaginary roots $x = i\omega^*$, with $\omega^* > 0$.

$$U_1\omega^{*2} - U_3 = Q_2 \cos(2\omega^*\tau) - Q_1\omega^* \sin(2\omega^*\tau), \tag{4}$$

$$\omega^{*3} - U_2\omega^* = Q_1\omega^* \cos(2\omega^*\tau) - Q_2 \sin(2\omega^*\tau). \tag{5}$$

Thus, after squaring and adding the equations (4) & (5) with $\omega^{*2} = \rho$, we obtain

$$\rho^3 + K_1\rho^2 + K_2\rho + K_3 = 0. \tag{6}$$

We choose the parameters so that K_1, K_2, and K_3 are all greater than zero. As a result, we conclude that no positive solution to equation (6) exists, this proves the asymptotic stability of the disease free steady state of the delayed system in equation (2). □

The next result discusses the stability of the SAI delayed system in equation (2) near the infected steady state and critical time delay for Hopf Bifurcation.

Theorem 5. *Let τ_1 be the critical time delay preceding Hopf bifurcation. Then the infected steady state of the system in equation (2) is stable for $\tau \in [0, \tau_1)$, else unstable. As τ passes through the critical value, the periodic solutions bifurcate from this infected steady state.*

Proof. To prove the stability of the infectious steady state, we consider equation (6) with an assumption of $U_3^2 < Q_2^2$. Under this assumption, equation (6) has one positive root and two purely imaginary roots. Next, by solving equations (4) and (5), we get

$$\tau_1 = \frac{1}{2\omega^*} \arccos\left[\frac{Q_1\omega^{*2}\left(\omega^{*2} - U_2\right) + Q_2\left(\omega^{*2}U_1 - U_3\right)}{\omega^{*2}Q_1^2 + Q_2^2} \right] + \frac{2n\pi}{\omega^*}, n = 0, 1, 2, \cdots$$

Again, a simple analysis based on the assumption that $2\omega^2(U_3 - U_1\omega^2) > 0$, shows that

$$\left[\frac{d(\text{Re}(x))}{d\tau} \right] > 0, \tag{7}$$

at $\omega = \omega^*$ and $\tau = \tau_1$. Hence, from equation (7) it is observed that the imaginary axis is crossed by the solution curve of the characteristic equation (6), and the Hopf bifurcation occurs at $\tau = \tau_1 > 0$ [19]. According to the continuity principle, the steady state of the infection is locally asymptotically stable at $\tau < \tau_1$. □

The SV delayed model is discussed in the next section with the time delay parameter associated with vaccination rate and failure of vaccination rate.

4.2. SV delay model

The SV delay model is framed with the susceptible compartment(S) and vaccination compartment(V), and it is considered to analyze the relationship between the susceptible and vaccination compartment with a time delay parameter associated with the rate of vaccination and rate of failure of vaccination and is given by

$$\begin{aligned} \frac{dS}{dt} &= (1-q)\Lambda - \delta S(t-\tau) - \varphi S + \gamma_3 V(t-\tau), \\ \frac{dV}{dt} &= q\Lambda + \varphi S(t-\tau) - \delta V - \gamma_3 V(t-\tau). \end{aligned} \tag{8}$$

It is essential to provide an initial condition for defining the value of the solution prior to time $t = 0$. Here, the initial conditions are $S_0(\theta) = \phi_1(\theta) > 0, V_0(\theta) = \phi_2(\theta) > 0$, with $\theta \in [-\tau, 0]$. Here, $\phi_i \in C\left([-\tau, 0] \to \mathbb{R}_+\right)$, $i = 1, 2$, are known functions.

In the vector form, we can rewrite the system in equation (8) by setting $X \in (S, V)^T \in \mathbb{R}^2$ and

$$H(X) = \begin{pmatrix} H_1(X) \\ H_2(X) \end{pmatrix} = \begin{pmatrix} (1-q)\Lambda - \delta S(t-\tau) - \varphi S + \gamma_3 V(t-\tau) \\ q\Lambda + \varphi S(t-\tau) - \delta V - \gamma_3 V(t-\tau) \end{pmatrix},$$

where $H : C_+ \to \mathbb{R}^2$ and $H \in C^\infty\left(\mathbb{R}^2\right)$. Hence, the delayed system in equation (8) becomes

$$\frac{dX_t(t)}{dt} = H\left(X_t\right),$$

where $X_t(\theta) = X(t+\theta)$. The following theorem describes the feasible region of the delayed system in equation (8).

Theorem 6. *The solutions of delayed system in equation (8) are positively invariant.*

Proof. To prove the delayed system in equation (8) is positively invariant, we consider the total population as M(t) and define

$$M(t) = S(t) + V(t).$$

From the non-negativity of the solutions associated with susceptible and vaccinated compartments, it follows that

$$\frac{dM}{dt} = \Lambda - \delta\left(S(t) + V(t)\right) \leq \Lambda - \delta M(t).$$

This indicates that $M(t)$ is bounded.

Therefore, the feasible region of delayed system in equation (8) is defined by

$$\Delta = \left\{(S, V) \in \mathbb{R}_+^2 : S, V \geq 0\right\},$$

is positively invariant. □

Next, we will determine adequate conditions on the parameters in order to ensure the stability of the steady state of system in equation (8).

Theorem 7. *The steady state* $(E_* = (S^*, V^*))$ *of delayed system in equation (8) is linearly asymptotically stable for* $\tau \geq 0$.

Proof. To prove the stability of the steady state of the delayed system in equation (8) we will use the Routh-Hurwitz criterion. Let J2 denote the Jacobian of delayed system in equation (8) at steady state $E_* = (S^*, V^*)$. Upon linearizing the system in equation (8) at J2 = 0, we get

$$\begin{vmatrix} -\delta - \varphi e^{-x\tau} - x & \gamma_3 e^{-x\tau} \\ \varphi e^{-x\tau} & -\delta - \gamma_3 e^{-x\tau} - x \end{vmatrix} = 0. \tag{9}$$

We have derived the characteristic polynomial in equation (9) as

$$(x + \delta) + e^{-x\tau} (\varphi + \gamma_3) = 0.$$

The following system of equation can be derived if the characteristic polynomial in equation (3) has purely imaginary roots $x = i\omega^*$, with $\omega^* > 0$.

$$-\cos(\omega\tau) = \frac{\delta}{(\varphi + \gamma_3)}, \tag{10}$$

$$\sin(\omega\tau) = \frac{\omega}{(\varphi + \gamma_3)}. \tag{11}$$

Thus, after squaring and adding the equations (10) & (11) with $\omega = \rho$, we obtain

$$\rho + \delta^2 - (\varphi + \gamma_3)^2 = 0. \tag{12}$$

Choosing the parameters $\delta^2 > (\varphi + \gamma_3)^2$, we conclude that no positive solution to equation (12) exists and this establishes the asymptotic stability of the steady state of the delayed system in equation (8). □

Now we provide the results on the stability of SV delay system in equation (8) near the steady state and the critical time delay of Hopf Bifurcation.

Theorem 8. *The steady state of delayed system in equation (8) is stable with* $\tau \in [0, \tau_2)$, *otherwise unstable. Where* τ_2 *signifies the critical time delay preceding Hopf bifurcation. The periodic solutions bifurcate from this steady state, as* τ *passes through the critical value.*

Proof. To prove the stability of the steady state, we obtain from the transcendental system of equations (10) & (11) as

$$\tau_2 = \frac{1}{\omega} \arccos \left[\frac{-\delta}{(\varphi + \gamma_3)} \right].$$

Proceeding in a similar manner as in the previous subsection, we conclude that the equilibrium is stable locally asymptotically at $\tau < \tau_2$. □

5. Numerical results

This section discusses the numerical analysis of proposed mathematical models and the verification of obtained analytical results. We analyze the behaviour of asymptomatic(A), infectious(I), and vaccinated(V) populations in the deterministic model for distinct values of R_0 and the success/failure rate of vaccination. Again, adding a small random perturbation, we discuss the difference in deterministic and stochastic behaviours. Also, we analyze both SAI delay and SV delay models for distinct values of the time delay parameter (τ) and used Python to perform the numerical simulations. The initial condition $(S_0, I_0, A_0, V_0) = (970, 10, 15, 5)$ kept fixed unless it is mentioned. The value of $\Lambda = 100$, and $\delta = 0.1$ are also fixed.

Fig. 1(a) and 1(b) explore the characteristics of asymptomatic and infectious populations. It has been observed that when the basic reproduction number (R_0) is less than 1, the number of asymptotic and infectious individuals tends to diminish and eventually reaches zero. Therefore, the deterministic model ultimately converges towards a state of disease free equilibrium. On the contrary, the number of individuals in the infectious population increases and stays stable with a positive value for $R_0 > 1$. Hence the deterministic model reaches endemic equilibrium for $R_0 > 1$. From the above figures, it is seen that the disease free equilibrium is stable for $R_0 < 1$ as established analytically in section-3 and the endemic equilibrium is stable for $R_0 > 1$.

Fig. 2 depicts the population variation in infected and vaccinated populations over time, along with various rates of success/failure of vaccination. The failure of vaccination rates is considered as 0.2 and 0.3 in Fig. 2(a) and 2(b), respectively. It is seen that as the vaccination rate rises, there is a decline in the infected population. Hence, to prevent the population from being infected, it is
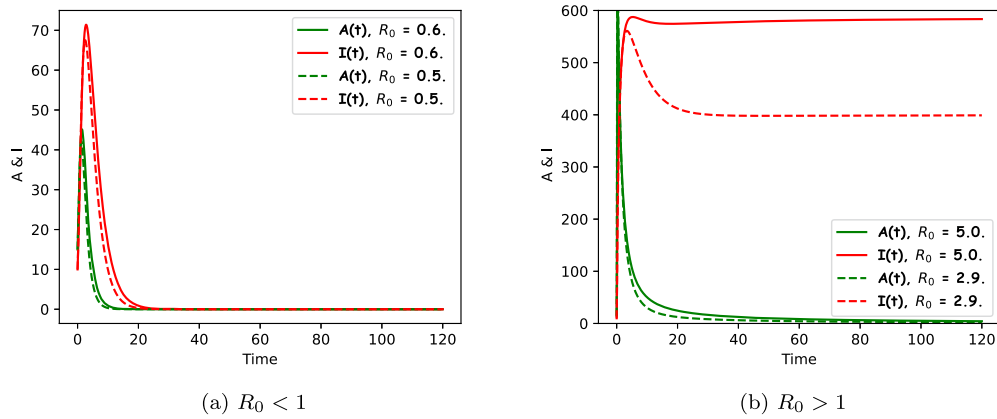
(a) $R_0 < 1$

(b) $R_0 > 1$

Fig. 1. Behaviour of A and I for the system in equation (1) with (a) λ = 0.6 & 0.7, q = 0.8, β = 0.002 & 0.002, φ = 0.6 & 0.7, γ_1 = 0.6 & 0.6, γ_2 = 0.7 & 0.7, γ_3 = 0.2 & 0.1, σ = 0.01 and (b) λ = 0.8 & 0.8, q = 0.8, β = 0.02 & 0.02, φ = 0.8 & 0.8, γ_1 = 0.3 & 0.6, γ_2 = 0.7 & 0.7, γ_3 = 0.2 & 0.2 and σ = 0.01.
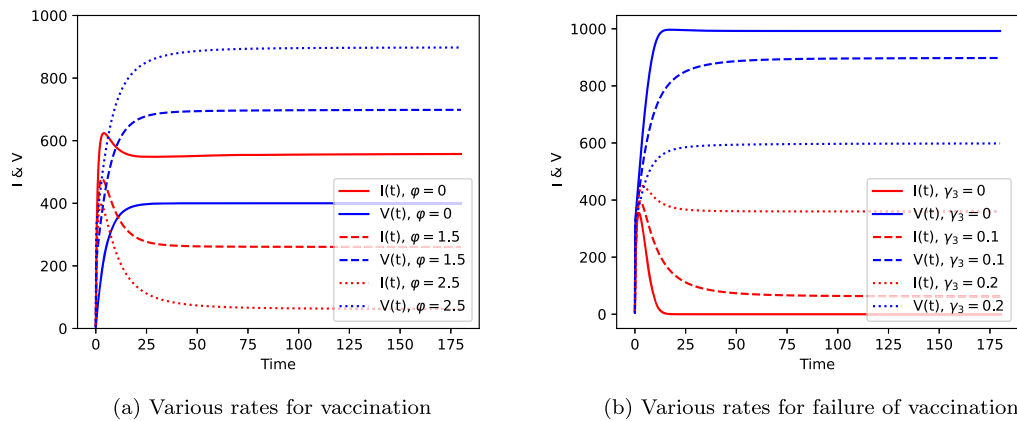

(a) Various rates for vaccination

(b) Various rates for failure of vaccination

Fig. 2. Behaviour of I and V for the system in equation (1) with q = 0.8, β = 0.02, λ = 0.8, γ_1 = 0.3, and γ_2 = 0.7.

(a) Infectious

(b) Vaccination
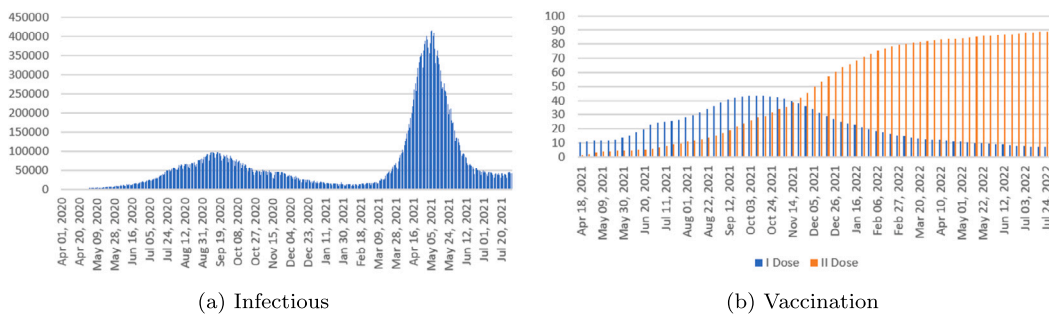
Fig. 3. Instances of Covid-19 every day in India. For the time period from April 18-2020 to July 24-2021, the actual numbers of infected patients and vaccinated individuals are clearly depicted. The data is derived from Worldometer and Vaccine Tracker.

essential to maintain a high vaccination rate and a low vaccination failure rate. The effect of vaccination on the infectious curve is shown in Fig. 3(a) and 3(b) based on data (https://www.worldometers.info/coronavirus/country/india/ and https://rb.gy/t4ufp). The peak of wave 1 is less than expected since control measures like lockdown and sanitizing are strictly enforced. As time passes, the efficiency of these control measures gets gradually less effective as preserving a sustainable economic environment is challenging. During wave 2, the vaccination overcame all other related measures and was essential in halting the rise of the infectious curve. When the percentage of the population that has received both vaccine doses increases, the infectious curve declines. In Fig. 4, in order to align the system in equation (1) with the current pandemic situation, we use the daily data in https://www.worldometers.info/coronavirus/country/india/ and https://rb.gy/t4ufp, regarding the number of infected individuals and vaccinated population in India between August 28, 2021, and November 8, 2021. We solely focus on the number of infected individuals and the percentage of vaccinated individuals during the decline of the second wave of Covid-19 in India. Fig. 4a indicates a decline in the number of
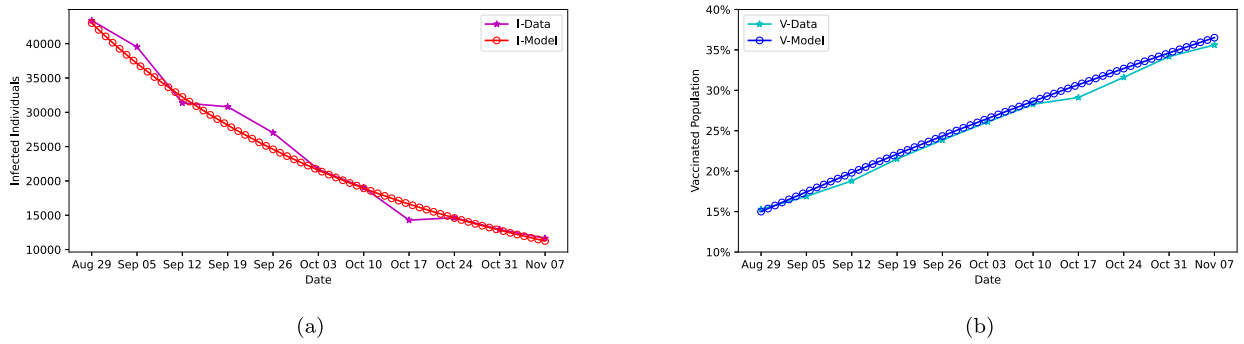
(a)

(b)

Fig. 4. The data in Fig. 3(a-b) is compared to the system in equation (1) to assess the impact of COVID-19 vaccination on infected individuals.
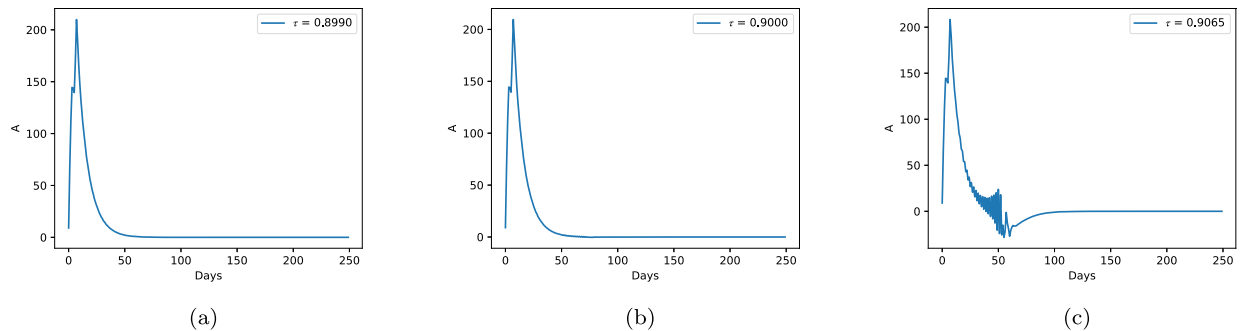

(a)

(b)

(c)

Fig. 5. Behaviour of Asymptomatic compartment for various values of time delay parameter (τ) with $q = 0.8$, $\lambda = 0.8$, $\beta = 0.02$, $\varphi = 0.8$, $\gamma_1 = 0.6$, $\gamma_2 = 0.7$ and $\gamma_3 = 0.1$.
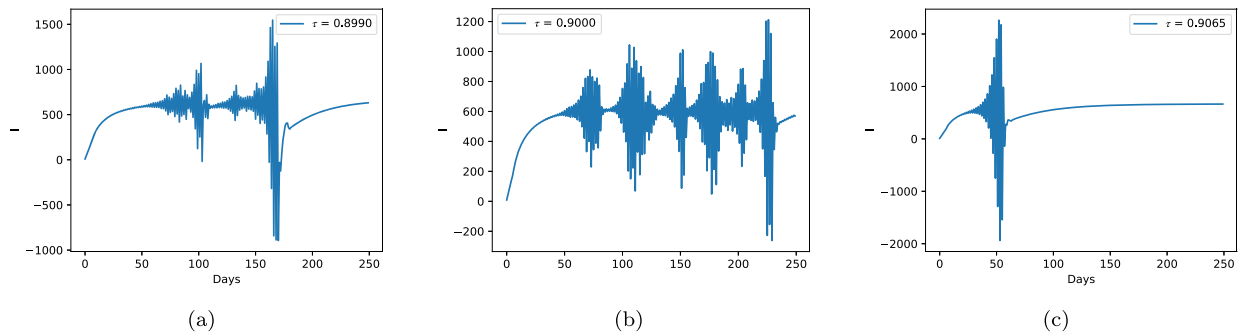

(a)

(b)

(c)

Fig. 6. Behaviour of Infectious compartment for different values of time delay parameter (τ) with $q = 0.8$, $\lambda = 0.8$, $\beta = 0.02$, $\varphi = 0.8$, $\gamma_1 = 0.6$, $\gamma_2 = 0.7$ and $\gamma_3 = 0.1$.

infected individuals over time, accompanied by an increase in the percentage of vaccination in Fig. 4b. Moreover, this result supports the notion that an increase in vaccination rates within the population is crucial in reducing the transmission of the disease. The initial condition from here is fixed as $(S_0, I_0, A_0, V_0) = (980, 9, 9, 2)$, to study the system in equation (2) and system in equation (8) numerically. From Fig. 5(a-c), it is observed that there is a variation in the asymptotic population for some values of the time delay parameter. It is also seen that the asymptotic solution approaches zero and remains at endemic equilibrium. From Fig. 6(a-c), we found the fluctuation or bifurcation of the infectious curve is not relevant to the increasing values of the time delay parameter, whereas the higher range of fluctuation occurs for periodic values of time delay parameter (τ) as discussed in system in equation (2).

From Fig. 7, it is observed that the susceptible population decreases whenever the vaccination population increases. As the rate of vaccination in the susceptible population is higher, with less possibility of failure of vaccination, the population rapidly moves from susceptible to the vaccinated compartment and remains stable. The impact of the time delay parameter (τ) is seen as a slight bifurcation in both the susceptible and vaccinated population before reaching equilibrium. Since both the vaccination rate and failure of vaccination rate are positive regardless of high or low, the population does not remain cent percent vaccinated. So, the populations of susceptible and vaccinated are greater than zero in the equilibrium.

Fig. 8 is plotted to study the nature of the solution with higher values of time delay parameter (τ). It is observed that at any time t, there is a decrease in a susceptible population whenever the vaccinated population increases. As the value of the time delay parameter (τ) increases, periodic solution occurs with a reduced range of fluctuation till the curve reaches the equilibrium. The value
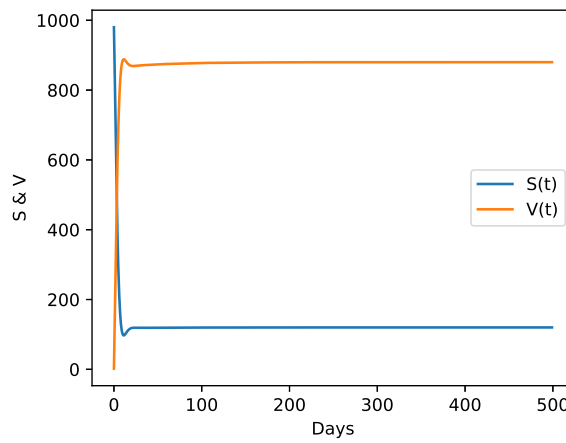
Fig. 7. Behaviour of susceptible and vaccination compartments for time delay parameter ($\tau = 0.5$) with $q = 0.8$, $\lambda = 0.8$, $\beta = 0.02$, $\varphi = 0.8$, $\gamma_1 = 0.6$, $\gamma_2 = 0.7$ and $\gamma_3 = 0.1$.
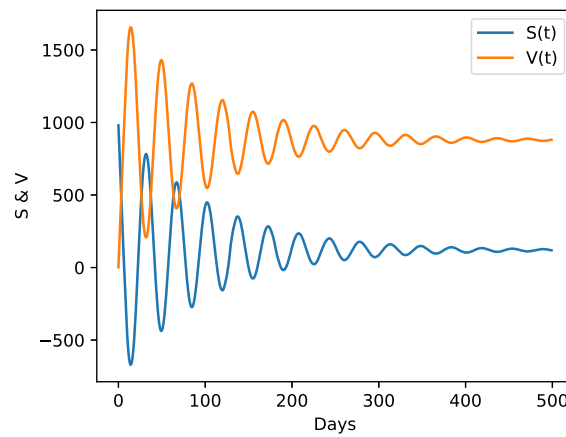

Fig. 8. Behaviour of susceptible and vaccination compartments for time delay parameter ($\tau = 1.6317$) with $q = 0.8$, $\lambda = 0.8$, $\beta = 0.02$, $\varphi = 0.8$, $\gamma_1 = 0.6$, $\gamma_2 = 0.7$ and $\gamma_3 = 0.1$.

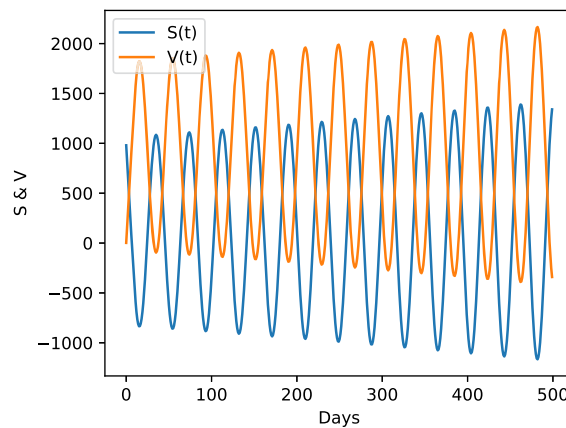**Fig. 9.** Behaviour of susceptible and vaccination compartments for time delay parameter ($\tau = 1.8807$) with $q = 0.8$, $\beta = 0.02$, $\varphi = 0.8$, $\lambda = 0.8$, $\gamma_1 = 0.6$, $\gamma_2 = 0.7$ and $\gamma_3 = 0.1$.

of the time delay parameter (τ) falls on the stable interval discussed in the system in equation (8) and hence, attracts the solutions toward the equilibrium.

We now analyze the behaviour of the solutions of the system in equation (8) with a time delay parameter (τ) near the critical time delay. Fig. 9 illustrates the periodic solutions bifurcate from this equilibrium as the time delay parameter (τ) higher than the critical

value, $\tau = 1.8806$, as discussed in the system in equation (8). In contradiction to the solutions in the previous Figure, we found, the amplitude increases over time with a constant wavelength, as the time delay parameter (τ) passes the critical time delay value, the periodic solutions bifurcate from equilibrium. The increasing fluctuation in the solutions concludes that the system in equation (8) does not reach equilibrium, and hence, it becomes unstable. From the above discussion, it is easy to see that the model is stable near the equilibrium with the time delay parameter less than the critical value at which Hopf Bifurcation occurs, as given in the system in equation (8), else the system in equation (8) becomes unstable.

6. Discussion

This article examines and analyses a mathematical model that more accurately depicts the evolution of Covid-19 disease, including the compartment for vaccinations. The assessment of disease severity is significant in determining the basic reproduction number. A Lyapunov function is formulated to evaluate the stability of the deterministic model. The numerical simulation demonstrates a significant influence of vaccination. We found that the disease free equilibrium remains stable for $R_0 < 1$ and unstable for $R_0 > 1$. Furthermore, it is assumed through numerical simulation that the stable endemic equilibrium exists for $R_0 > 1$. Then we split the model with a time delay parameter to observe the stability and Hopf bifurcation. We found that the delayed systems are stable with a time delay parameter less than the critical value at which Hopf Bifurcation takes place. Our work provides a theoretical basis for how the vaccinated population affects the pandemic, hence leading to prudent decisions and measures to control pandemics such as Covid-19. The constraint in the suggested model is the assumption of homogeneous interactions among populations transitioning to the compartment, as well as the assumption of natural and equal death rates. Future research in this field involves incorporating a stochastic perturbation and a more realistic scenario by utilizing data to incorporate the impact of lockdown restrictions and social mobility on the spread of infections. This will enable us to effectively address the issue of controlling measures and mitigating epidemics while considering their interdependence.

CRediT authorship contribution statement

Mohammed Salman: Conceptualization, Data curation, Investigation, Validation, Writing – original draft. **Sanjay Kumar Mohanty:** Conceptualization, Data curation, Investigation, Supervision, Validation, Writing – original draft. **Chittaranjan Nayak:** Investigation, Validation, Writing – review & editing. **Sachin Kumar:** Investigation, Validation, Writing – review & editing.

Declaration of competing interest

The authors declare that they have no known competing financial interests or personal relationships that could have appeared to influence the work reported in this paper.

Data availability

Data will be made available on request from the corresponding authors.

Acknowledgements

Appendix A

In section 3, we discuss the stability of disease free equilibrium through Lyapunov function. Here, we included a few additional calculation steps.

$$
\begin{aligned}
\frac{dL_1}{dt} &= C_0 \left[\frac{\Lambda\beta\mu(\delta(1-q)+\gamma_3)}{\delta C_0(\delta+\varphi+\gamma_3)(\delta+\gamma_1+\lambda)} A + \frac{\dot{A}}{C_0(\delta+\gamma_1+\lambda)} + I + \frac{\dot{I}}{\delta+\gamma_2} \right] \\
&= \frac{\Lambda\beta\mu(\delta(1-q)+\gamma_3)}{\delta(\delta+\varphi+\gamma_3)(\delta+\gamma_1+\lambda)} A + \frac{\mu\beta SA - \delta A - \lambda A - \gamma_1 A}{\delta+\gamma_1+\lambda} + C_0 I \\
&\quad + C_0 \left[\frac{\beta SI + \lambda A - \delta I - \gamma_2 I}{\delta+\gamma_2} \right], \\
&= \frac{\Lambda\beta\mu(\delta(1-q)+\gamma_3)}{\delta(\delta+\varphi+\gamma_3)(\delta+\gamma_1+\lambda)} A + \frac{(\mu\beta S - \delta - \lambda - \gamma_1)A}{\delta+\gamma_1+\lambda} + C_0 I \\
&\quad + C_0 \left[\frac{(\beta S - \delta - \gamma_2)I + \lambda A}{\delta+\gamma_2} \right] \\
&= \frac{\Lambda\beta\mu(\delta(1-q)+\gamma_3)}{\delta(\delta+\varphi+\gamma_3)(\delta+\gamma_1+\lambda)} A + \frac{\mu\beta SA}{\delta+\gamma_1+\lambda} - \frac{(\delta+\lambda+\gamma_1)A}{\delta+\gamma_1+\lambda}
\end{aligned}
$$

$$+ C_0 I + C_0 \left[\frac{(\beta S - \delta - \gamma_2)I + \lambda A}{\delta + \gamma_2} \right]$$

$$= \left[\frac{\Lambda \beta \mu (\delta(1-q) + \gamma_3)}{\delta(\delta + \varphi + \gamma_3)(\delta + \gamma_1 + \lambda)} - 1 \right] A + C_0 \left[\frac{\beta S I}{\delta + \gamma_2} + \frac{\lambda A}{\delta + \gamma_2} \right]$$

$$+ \left[\frac{\mu \beta S A}{\delta + \gamma_1 + \lambda} \right]$$

$$= \left[R_0 - 1 \right] A + C_0 \left[\frac{\mu \beta S A}{C_0(\delta + \gamma_1 + \lambda)} + \frac{\beta S I}{\delta + \gamma_2} + \frac{\lambda A}{\delta + \gamma_2} \right].$$

References

[1] W.O. Kermack, A.G. McKendrick, A contribution to the mathematical theory of epidemics, Proc. R. Soc. Lond. Ser. A 115 (772) (1927) 700–721.

[2] P. Van den Driessche, J. Watmugh, Reproduction numbers and sub-threshold endemic equilibria for compartmental models of disease transmission, Math. Biosci. 180 (1–2) (2002) 29–48.

[3] M.N. Hassan, M.S. Mahmud, K.F. Nipa, M. Kamrujjaman, Mathematical modeling and Covid-19 forecast in Texas USA: a prediction model analysis and the probability of disease outbreak, Disaster Med. Public Health Prep. 17 (2023) e19.

[4] C.M. Kribs-Zaleta, J.X. Velasco-Hernández, A simple vaccination model with multiple endemic states, Math. Biosci. 164 (2) (2000) 183–201.

[5] L. Mpinganzima, J.M. Ntaganda, W. Banzi, J.P. Muhirwa, B.K. Nannyonga, J. Niyobuhungiro, I.S. Mbalawata, Compartmental mathematical modelling of dynamic transmissions of COVID-19 in Rwanda, IJID Reg. (2023).

[6] D. Okuonghae, A. Omame, Analysis of a mathematical model for COVID-19 population dynamics in Lagos, Nigeria, Chaos Solitons Fractals 139 (2020) 110032.

[7] L.M. Mwangi, W.N. Mutuku, Mathematical modelling on impact of interventions in the spread of Covid-19 in Kenya, J. Adv. Math. Comput. Sci. 38 (1) (2023) 1–19.

[8] O.J. Watson, G. Barnsley, J. Toor, A.B. Hogan, P. Winskill, A.C. Ghani, Global impact of the first year of COVID-19 vaccination: a mathematical modelling study, Lancet Infect. Dis. 22 (9) (2022) 1293–1302.

[9] Z. Shuai, P. Van den Driessche, Global stability of infectious disease models using Lyapunov functions, SIAM J. Appl. Math. 73 (4) (2013) 1513–1532.

[10] B. Kammegne, K. Oshinubi, O. Babasola, O.J. Peter, O.B. Longe, R.B. Ogunrinde, J. Demongeot, Mathematical modelling of the spatial distribution of a COVID-19 outbreak with vaccination using diffusion equation, Pathogens 12 (1) (2023) 88.

[11] P. De Leenheer, D. Aeyels, Stabilization of positive linear systems, Syst. Control Lett. 44 (4) (2001) 259–271.

[12] X. Guan, F. Yang, Y. Cai, W. Wang, Global stability of an influenza A model with vaccination, Appl. Math. Lett. 134 (2022) 108322.

[13] A. Omame, D. Okuonghae, U.K. Nwajeri, C.P. Onyenegecha, A fractional-order multi-vaccination model for COVID-19 with non-singular kernel, Alex. Eng. J. 61 (8) (2022) 6089–6104.

[14] M.M. Ojo, O.J. Peter, E.F.D. Goufo, K.S. Nisar, A mathematical model for the co-dynamics of COVID-19 and tuberculosis, Math. Comput. Simul. (2023).

[15] A. Omame, M. Abbas, Modeling SARS-CoV-2 and HBV co-dynamics with optimal control, Phys. A, Stat. Mech. Appl. 615 (2023) 128607.

[16] A. Omame, M. Abbas, A. Din, Global asymptotic stability, extinction and ergodic stationary distribution in a stochastic model for dual variants of SARS-CoV-2, Math. Comput. Simul. 204 (2023) 302–336.

[17] V.V. Albani, R.A.S. Albani, E. Massad, J.P. Zubelli, Nowcasting and forecasting COVID-19 waves: the recursive and stochastic nature of transmission, R. Soc. Open Sci. 9 (8) (2022) 220489.

[18] Á. Leitao, C. Vázquez, The stochastic θ-SEIHRD model: adding randomness to the COVID-19 spread, Commun. Nonlinear Sci. Numer. Simul. 115 (2022) 106731.

[19] S. Tyagi, S.C. Martha, S. Abbas, A. Debbouche, Mathematical modeling and analysis for controlling the spread of infectious diseases, Chaos Solitons Fractals 144 (2021) 110707.

[20] X.Z. Meng, L.S. Chen, Z.T. Song, Global dynamics behaviors for new delay SEIR epidemic disease model with vertical transmission and pulse vaccination, Appl. Math. Mech. 28 (9) (2007) 1259–1271.

[21] G. Röst, SEIR epidemiological model with varying infectivity and infinite delay, Math. Biosci. Eng. 5 (2) (2008) 389–402.

[22] R. Xu, Z. Ma, Global stability of a delayed SEIRS epidemic model with saturation incidence rate, Nonlinear Dyn. 61 (1–2) (2010) 229–239.

[23] G. Dagasso, J. Urban, M. Kwiatkowska, Incorporating time delays in the mathematical modelling of the human immune response in viral infections, Proc. Comput. Sci. 185 (2021) 144–151.

[24] I. Ahmed, G.U. Modu, A. Yusuf, P. Kumam, I. Yusuf, A mathematical model of Coronavirus Disease (COVID-19) containing asymptomatic and symptomatic classes, Results Phys. 21 (2021) 103776.

[25] Y. Jin, W. Wang, S. Xiao, An SIRS model with a nonlinear incidence rate, Chaos Solitons Fractals 34 (5) (2007) 1482–1497.

[26] O. Diekmann, J.A.P. Heesterbeek, M.G. Roberts, The construction of next-generation matrices for compartmental epidemic models, J. R. Soc. Interface 7 (47) (2010) 873–885.